AIAA JOURNAL
Vol. 47, No. 7, July 2009

Polymer Nanofabric Interleaved Composite Laminates

Kunigal Shivakumar,* Shivalingappa Lingaiah,† Huanchun Chen,‡ Paul Akangah,§ and Gowthaman Swaminathan¶
North Carolina Agricultural and Technical State University, Greensboro, North Carolina 27411
and
Larry Russell Jr.**
U.S. Army Research Office, Research Triangle Park, North Carolina 27709

DOI: 10.2514/1.41791

The concept of electrospun polymer nanofiber fabric interleaving to enhance dynamic properties, impact damage resistance, fracture toughness and resistance, and delamination onset life was evaluated. Polymer nanofabric interleaving increased the laminate thickness and weight by an order of 1%, and its impact on in-plane mechanical properties of the composite laminate would be statistically zero. On the other hand, its influence on interlaminar fracture toughness and resistance, impact damage resistance, and damping is substantial. Results of this study showed that interleaving AS4/3501-6 composite laminate increased the damping by 13%, reduced the impact damage size to one-third, increased fracture toughness and resistance by 1.5 times and one-third, respectively, significantly increased delamination onset life, and increased the fatigue threshold energy release rate by two-thirds. These improvements are comparable to that of the commercial T800H/3900-2 composite but with no thickness increase penalty, loss of in-plane properties, or multiple glass transition temperatures.

Nomenclature

A	=	cross-sectional area of cantilever beam, m^2
a_{IC}	=	initial delamination length for the fracture test
$a(t)$	=	acceleration at any time t
a_0	=	initial delamination length
da	=	delamination extension
E'	=	material storage modulus, Pa
E''	=	material loss modulus, Pa
$E(t)$	=	instantaneous energy at any time t
G_I	=	mode I energy release rate
G_{IC}	=	initiation mode I fracture toughness
$G_{I\max}$	=	maximum cyclic mode I energy release rate
G_{IR}	=	plateaued mode I fracture resistance
G_R	=	fracture resistance
g	=	acceleration due to gravity, 9.81 m/s^2
L	=	length of the cantilever beam
M	=	effective mass of the impactor system
M_a	=	mass of the impactor and the accelerometer system
$N_{1\%}$	=	number of cycles for 1% compliance increase
$P(t)$	=	instantaneous impact force, N
R	=	ratio of minimum and maximum cyclic displacement $\delta_{I\min}/\delta_{I\max}$
T_g	=	glass transition temperature
t	=	time, s
$\tan\delta$	=	damping factor
V_0	=	initial velocity of the impactor at the time of impact
Δ	=	delamination length correction parameter
δ_{IC}	=	critical load-point displacement when the delamination starts to grow in the fracture test
$\delta_{I\max}$	=	maximum value of cyclic displacement
$\delta_{I\min}$	=	minimum value of cyclic displacement
ρ	=	mass density of the cantilever beam

Presented at the 50th AIAA/ASME/ASCE/AHS/ASC Structures, Structural Dynamics, and Materials Conference, Palm Springs Convention Center/Wyndham Palm Springs, CA, 2–7 May 2009; received 24 October 2008; revision received 17 March 2009; accepted for publication 23 March 2009.

*Research Professor and Director, Department of Mechanical and Chemical Engineering, Center for Composite Materials Research. Associate Fellow AIAA.
†Senior Research Scientist, Department of Mechanical and Chemical Engineering, Center for Composite Materials Research. Member AIAA.
‡Research Associate, Department of Mechanical and Chemical Engineering, Center for Composite Materials Research.
§Graduate Student, Department of Mechanical and Chemical Engineering, Center for Composite Materials Research.
¶Graduate Student, Department of Mechanical and Chemical Engineering, Center for Composite Materials Research. Member AIAA.
**Physical Scientist, Environmental Sciences Division.

I. Introduction

THE primary limitation of composite laminates is the poor interlaminar strength and toughness, which causes delamination [1] and ultimately the structural failure. Interlaminar stresses due to mismatch of anisotropic mechanical and thermal properties occur at the free edges, joints, matrix cracks, and under out-of-plane loading. Analysis of edge stress [2] and delamination models [3] showed a concentration of interlaminar shear and transverse stresses near the edges and cracks. Such high stresses combined with weak interlaminar properties cause delamination in composite laminates. A number of methods to prevent delamination have been developed over the years [4–12]. These include matrix toughening [7], optimization of stacking sequence [8], laminate stitching [9,10], use of braided fabric [10], edge-cap reinforcement [11], critical ply termination [12], and replacement of a stiff ply by a softer ply. Designs to reduce delamination resulted in significant increase in cost, weight, or loss of in-plane properties. An approach that is attractive to reduce the preceding problems is by ductile interleaving [13]. Interleaving is an old concept that was used in the aircraft industry to enhance acoustic damping and interrupt fatigue crack propagation in metallic structures. Recently, Toray Corporation developed a thermoplastic particle interleaved prepreg, T800H/3900-2, which has become a choice composite in the Boeing 777 because of its superior impact damage resistance and threefold increase in initiation fracture toughness G_{IC} [14]. The primary drawbacks of particle interleaved composites are increased laminate thickness (~20%), decreased in-plane stiffness (15–20%) and strength, and potentially lowering of T_g. The preceding problems could be potentially eliminated/reduced and, furthermore, the

composite can be multifunctionalized (example, electrical properties) by the use of electrospun nonwoven nanofiber fabric interleaving. By proper choice of nanofiber size and material, large surface areas of adhesion and torturous fracture modes could be created to increase the toughness.

Electrospinning of solvated or melt polymers [15] was developed in the 1940s and has been used in the medical industry for several decades. This technology is becoming very attractive for a number of applications, including drug delivery, cosmetics, and tissue engineering [16]. Shivakumar and Lingaiah [17] and Lingaiah et al. [18] had an opportunity to develop electrospinning for fabricating high tear strength and ultralightweight membranes for artificial dragonfly wings [17,18]. Membranes were made of nonwoven Nylon-66 nanofibers of diameters ranging from 50–200 nm and several inches long. These fibers have extremely high specific surface area and excellent adhesion to epoxy matrix. The idea that is explored here is that, by addition of a small amount of high elongation polymer nanofibers, the epoxy matrix can be toughened without loss of in-plane properties.

The objective of this paper is to explore the concept of electrospun polymer nanofabric interleaving and its impact on damping factor, interlaminar fracture toughness, and impact damage tolerance of laminated composites. Plain and nanofabric interleaved AS4/3501-6 as well as T800H/3900-2 composite laminates were fabricated and tested for improved material damping, resistance to low velocity impact damage, mode I fracture toughness, and delamination onset life. The results of plain AS4/3501-6 and nanofabric interleaved AS4/3501-6 (AS4/3501-6_IN) composites are compared with each other to assess the effect of interleaving and with the commercial thermoplastic particles interleaved T800H/3900-2 composite.

II. Approach

A. Materials

AS4/3501-6 prepreg supplied by Hexcel Composites was chosen as the base material to improve its dynamic, damage tolerance, and toughness properties by interleaving. Nylon-66 supplied by DuPont Company (Zytel 101, MW $= 20,000$ g/mol) was selected to prepare the nonwoven nanofabric by electrospinning. Nylon-66 has extremely high elongation to fracture, readily bonded with epoxy, and high melting/softening temperature (250°C) compared to the AS4/3501-6 cure temperature (177°C). Thus, the Nylon-66 fibers would be unaffected during the cure conditions of the composite. T800H/3900-2 prepreg was supplied by Toray Composites, Inc. This prepreg was made by sprinkling fine thermoplastic (polyamide) particles on the T800H/3631 prepreg. The thickness of the thermoplastic particles interlayer was about 30 μm and the bare prepreg thickness was about 160 μm [19]. This amount is about a 20% increase in thickness. Based on the mechanics of composite materials, this thickness increase amounts to nearly the same amount loss of in-plane stiffness and strength.

B. Electrospinning of Nylon-66

Electrospinning uses an electrostatic force to spin fibers from a polymeric solution. The Nylon-66 was dissolved in a mixture of formic acid and chloroform with a weight ratio of 75/25 [17,18] by vigorously stirring at room temperature until the mixture became a homogeneous solution. The solution was transferred to a syringe with a fine needle. The tip of the needle and collector are at a potential of tens of kilovolts. An electric field induces a charge on the liquid surface at the tip of the needle. Mutual repulsion of charge causes a force directly opposite to the surface tension. As the intensity of the electric field is increased, the hemispherical fluid at the tip of the needle elongates to form a conical shape known as the Taylor cone. With increasing electric field between the needle and the target, at a critical value, a charged jet of fluid is ejected from the tip of the Taylor cone. The discharged jet undergoes a whipping action that further elongates the polymer and the repulsive electrostatic field in the fluid splits the jet into fine submicron fibers that are collected on a grounded metal collector or drum. The polymer fiber diameter and their alignment depends on the type and concentration of polymer in the solution, voltage, flow rate, needle diameter, distance between needle and collector drum, and the type of collector. Rotating drum electrospinning is illustrated in Figs. 1a and 1b and the scanning electron microscope (SEM) image of the electrospun fabric is shown in Fig. 1c. The fibers' diameter ranged from 75 to 250 nm. The electrospinning parameters used were as follows: 12% Nylon-66 concentration, 35 kV voltage, 20.3 cm distance between needle and collector, 0.25 mm needle diameter, 1 ml/h flow rate, 3.0 m/s drum linear speed, and 120 min spinning duration. The areal density of the fabric ranged from 1.6 to 2.0 g/m^2, a ply of AS4/3501-6 is 150 g/m^2, which results in the nanofabric weight percentage between 1 and 1.4%.

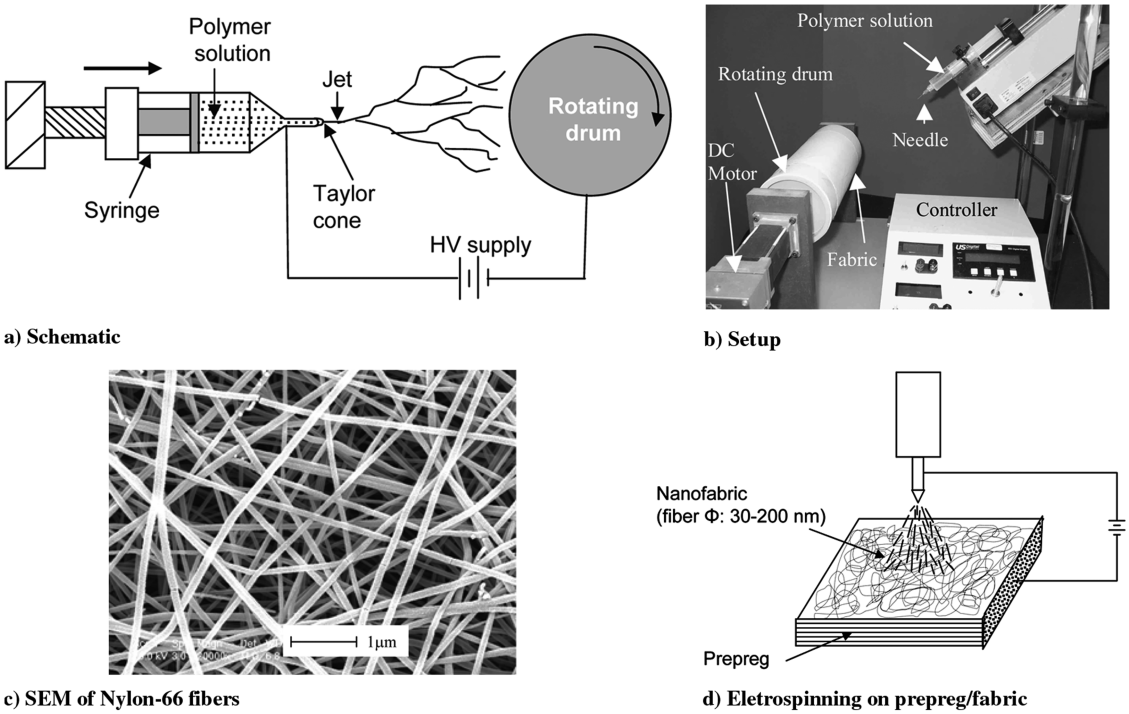

a) Schematic

b) Setup

c) SEM of Nylon-66 fibers

d) Eletrospinning on prepreg/fabric

Fig. 1 Electrospinning and morphology of electrospun Nylon-66 fibers.

C. Fabrication of Panels and Test Specimens

Three different tests required three different types of panels and stacking sequences. Accordingly, unidirectional (0° deg) laminates were fabricated for dynamic mechanical analysis (DMA), and fracture and delamination onset life tests, and a quasi-isotropic laminate of $(-45/90/45/0)_{2S}$ stacking sequence was fabricated for impact testing. Interleaved panels for DMA and impact tests were 6-ply and 16-ply thick, respectively, and were made by placing one layer of nanofiber fabric over each of the prepreg plies except for the last layer. Midplane delaminated 20-ply unidirectional panels were made for mode I fracture and fatigue delamination onset life tests. Here, the interleaved panels were made by placing two layers of nanofiber fabrics between the top and bottom 10 layers of prepreg. In a manufacturing setup, one could directly electrospin nanofibers on a prepreg or on the reinforcing fabric (Fig. 1d). In addition to interleaved panels, plain AS4/3501-6 panels were also made of same stacking sequences to generate the baseline data. A 16-ply quasi-isotropic T800H/3900-2 composite laminate was also fabricated for impact testing and its thickness was 2.95 mm. These panels were made in an autoclave as per the guidance provided by the prepreg supplier. The average areal density of a single layer of nanofabric used for DMA, impact, and fracture test panels was 1.6, 1.7, and 1.5 g/m^2, respectively. The corresponding calculated thickness (based on the assumed density of 1.14 g/cc for Nylon-66) of the fabrics was 1.4, 1.5, and 1.3 μm, respectively. The average thickness of DMA, impact, and fracture test panels was 0.713, 2.18, and 2.7 mm for interleaved panels, whereas it was 0.70, 2.13, and 2.7 mm for plain panels. The areal weight difference between the interleaved and noninterleaved is about 1.4%.

III. Test

A. Dynamic Mechanical Analysis Test

Dynamic mechanical analysis tests were conducted to measure the glass transition temperature T_g and the material damping factor. Tests were conducted using PerkinElmer DMA 7 equipment in a three-point bending mode. The test specimen's nominal dimensions were as follows: length 24 mm, span 20 mm, thickness 0.7 mm, and width 2 mm. Specimen preparation and DMA tests were conducted as per the guidance suggested by Swaminathan and Shivakumar [20]. The specimen was supported on two roller supports separated by 20 mm with a midspan load of 1 N exciting at 1 Hz. The test was conducted for a temperature range of 25–275°C, heated at 5°C/ min. The load and displacement response was recorded continuously as a function of temperature. From that data, the material storage modulus E' and loss modulus E'' were determined. Then, the damping factor $\tan\delta$ was calculated by taking the ratio of E'' and E' at any temperature. Tests were repeated for all specimens. Ambient (room) temperature data were used to calculate the damping factor.

B. Impact Test

Impact tests were conducted on quasi-isotropic laminates with a 50.8-mm-diam circular test section that was clamped to a rigid base. The test setup was fabricated by placing the square test specimen measuring 76.2 × 76.2 mm in between an upper steel plate of 142 × 132 × 10 mm and a bottom channel-section steel beam of nearly the same web thickness. Both the plate and the beam had a circular cutout section of 50.8 mm diameter. Centers of the plate and the holes were aligned and clamped together by six bolts tightened to a preset torque of 2.2 Nm. The impactor was a steel spherical ball having a diameter of 12.7 mm attached to a steel cantilever beam. The impactor is instrumented to measure acceleration. Figure 2 shows the schematic and photograph of the tester. Although this setup has the potential to cause repeated rebound impacts, its effect is ignored in this study.

The data acquisition system consists of an instrumented cantilever with a Kistler 8704B5000 accelerometer, which was in turn connected to a coupler, DL750 Scopecorder, and a PC. The DL750 Scopecorder is an advanced software-driven oscilloscope and was programmed to output acceleration data both in raw and smoothened (using the forward-moving average algorithm) formats. Data from the Scopecorder was transferred to a PC and then analyzed using Xviewer software.

After connecting the accelerometer to the digital oscilloscope and clamping the specimen, an impact test was conducted by pulling the impactor to a preset height and allowing it to strike the center of the test section. Tests were conducted at impact heights of 38.1 and 50.8 mm. Raw acceleration data, moving average smoothened acceleration data, and time were acquired continuously by the oscilloscope. By performing first and second numerical integration [21] of the raw acceleration data, respectively, velocity and displacement of the impactor were computed. Instantaneous impact force $P(t)$ was calculated by multiplying the effective mass M of the impactor system by the instantaneous acceleration $a(t)$. By integrating the force-displacement curve, impact energy $E(t)$ was calculated. The expressions for the impact force $P(t)$ at any time t is given by

$$P(t) = Ma(t) \tag{1}$$

where

$$M = 0.243\rho AL + M_a \tag{2}$$

and ρ is mass density, A is the cross-sectional area, and L is the length of the cantilever beam.

The first term in Eq. (2) is the effective mass of the cantilever beam, calculated by matching the first natural frequency of an equivalent spring-mass system to that of the cantilever beam [22]. The second term (M_a) in Eq. (2) is the mass of the impactor and the accelerometer system.

The expression for the impact energy $E(t)$ is given by

$$E(t) = \int_0^t \left\{ P(t) \int_0^t \left[V_0 - \int_0^t a(t)\,\mathrm{d}t \right] \mathrm{d}t \right\} \mathrm{d}t \tag{3}$$

Tests were repeated for all three materials: AS4/3501-6, AS4/3501-6_IN, and T800H/3900-2 composites. Impacted test specimens were c-scanned using Structrual Diagnostic, Inc. c-scan instruments to measure the gross damage area. Then the specimens were sectioned along the maximum damage length to measure through-the-thickness damage distribution.

C. Mode I Fracture and Delamination Onset Life Tests

The mode I fracture test was conducted using a double cantilever beam (DCB) specimen of 230-mm long, 20-mm wide, and 2.5-mm thick. The initial delamination length was about 50 mm. Figure 3 shows the specimen configuration and the loading. The fracture test

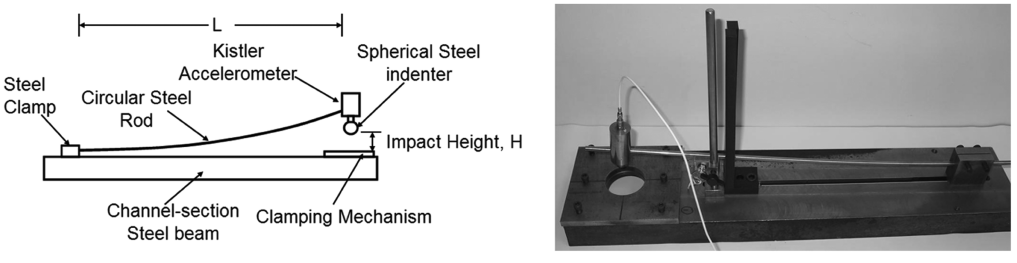

Fig. 2 Schematic and photograph of cantilever beam impact tester.

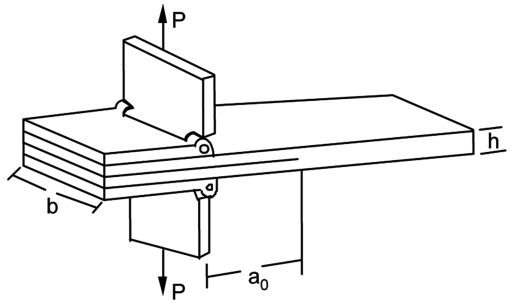

Fig. 3 Fracture and fatigue onset tests specimen configuration.

was conducted according to American Society for Testing and Materials (ASTM) Standard D5528 [23]. The test was carried out in an MTS Systems test machine using a 880 N (200 lb) load cell under displacement control at a constant crosshead rate of 1.3 mm/ min. Load, crosshead displacement, and the crack length a were recorded continuously during the test.

The energy release rate G_I was calculated from the modified beam theory [24]:

$$G_I = \frac{3P\delta}{2b(a + |\Delta|)} \tag{4}$$

where P is the load, δ is the load-point displacement, b is the specimen width, a is the delamination length, and Δ is the delamination length correction parameter for the not perfectly built-in condition of the DCB. The value of Δ is established after the test. Maximum load and the associated deflection δ at the initial delamination length a_0 was used to calculate the initiation fracture toughness G_{IC} of the material. For $a > a_0$, the G_I becomes G_R, fracture resistance. The G_R, once it becomes nearly constant, is called G_{IR}.

The mode I fatigue delamination growth onset life test was conducted according to ASTM D6115 [25] to obtain the fatigue delamination onset life $N_{1\%}$, number of cycles for 1% compliance increase. The test specimens had the same configuration as the fracture test. The test was conducted under displacement control with a loading ratio $R = \delta_{I\min}/\delta_{I\max} = 0.3$. Tests were conducted for different values of $G_{I\max}$. An equivalent maximum displacement $\delta_{I\max}$ equation was derived using the beam theory and the specimen similarity approach and is given by

$$\delta_{I\max} = \sqrt{\frac{G_{I\max}}{G_{IC}}}\left(\frac{a_0 + \Delta}{a_{IC} + \Delta}\right)^2 \delta_{IC} \tag{5}$$

where a_0 is the initial delamination length for the fatigue onset life test, a_{IC} is the initial delamination length of the fracture test used in this calculation, Δ is the delamination length correction parameter obtained from the fracture test, and δ_{IC} is the critical load-point displacement when the delamination starts to grow in the fracture test. The test specimen was cycled until the compliance increased by 1%. The fatigue delamination onset life $N_{1\%}$ was determined for different values of $G_{I\max}$ and from that data $G_{I\text{threshold}}$ was determined. The $G_{I\text{threshold}}$ is the $G_{I\max}$ required to increase 1% compliance in 1 million load cycles.

IV. Results and Discussion

A. Dynamic Mechanical Analysis Test

Figure 4 shows the plots of storage modulus E' and the damping factor tan δ versus temperature for plain and interleaved AS4/3501-6 composites and the T800H/3900-2 composite. The E' of plain and interleaved AS4/3501-6 and T800H/3900-2 composites was 128.1, 115.1, and 116.1 GPa, respectively. The 9% difference in modulus is typical of DMA tests, as observed in the literature [20]. The T_g determined as per the ASTM standard E1640-04 [26] was 195 and 191°C, for the plain and interleaved AS4/3501-6 composites, respectively. The difference between the two is within the expected

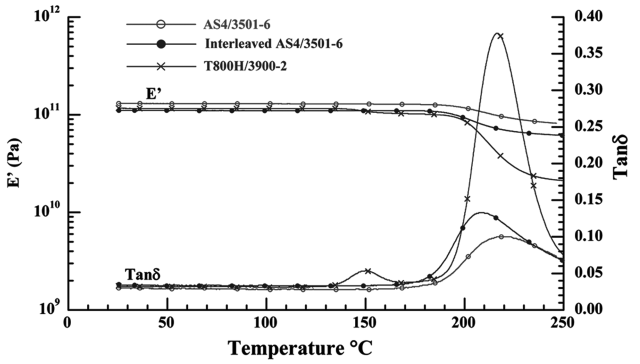

Fig. 4 Comparison of DMA profiles of AS4/3501-6 composites and T800H/3900-2 composite.

margin of error in the test data. The room temperature damping factors for the two materials were 0.030 and 0.034, respectively, with an increase of about 13% by adding about 1.4% thick nanofabric interleave.

The DMA test on the T800H/3900-2 material showed two values of T_g, one at 140°C and another at 198°C. The lower T_g is attributed to the softening of thermoplastic particles and the higher T_g is that of the base matrix. The damping factor of T800H/3900-2 is 0.037, which is about 23% larger than the AS4/3501-6 composite. Multiple T_g, particularly the lower value of the T800H/3900-2 composite, could be a concern to structural designers.

B. Impact Test

Figures 5 and 6 represent, respectively, impact force and energy versus time for plain and interleaved panels for impact heights of 38.1 and 50.8 mm. For $H = 38.1$ mm, $P(t)$ versus t is a nice smooth sinusoidal response, which is a characteristic of an undamaged specimen. However, for $H = 50.8$ mm, the plain AS4/3501-6 shows

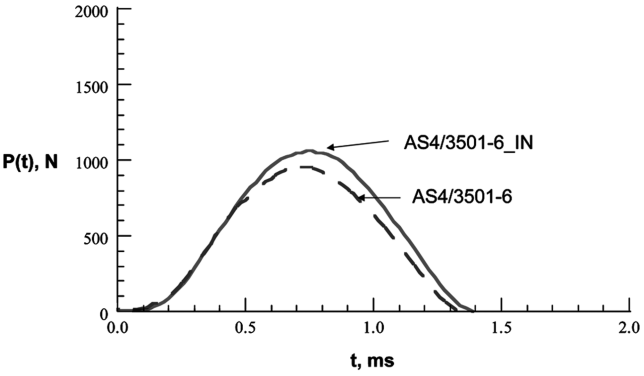

a) Impact force at impact height, H = 38.1 mm

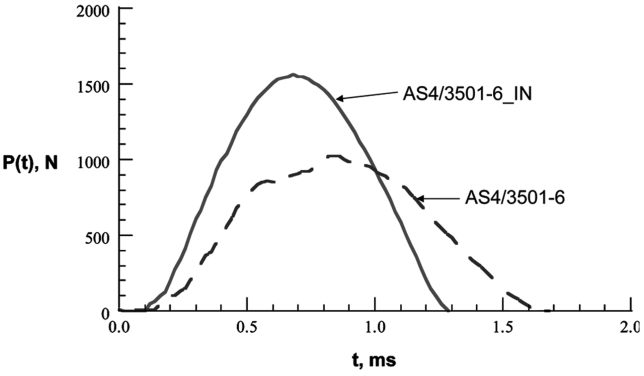

b) Impact force at impact height, H = 50.8 mm

Fig. 5 Impact force versus time for plain and interleaved AS4/3501-6 for two different impact heights.

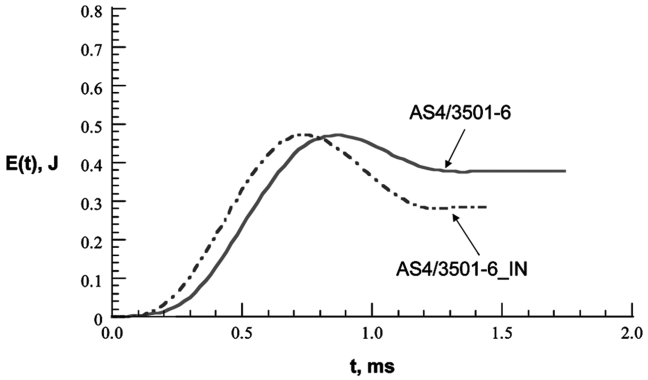

a) Impact energy at impact height, H = 38.1 mm

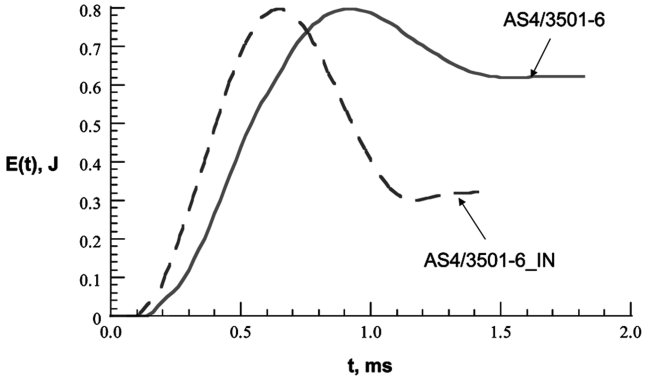

b) Impact energy at impact height, H = 50.8 mm

Fig. 6 Impact energy versus time for plain and interleaved AS4/3501-6 for two different impact heights.

a flat peak, an indication of damage during the impact event. Table 1 summarizes panel thickness, maximum impact force and energy, impact duration (which is the elapsed time between the impact incident and when the impact force just turns zero or negative), and damage area of plain and interleaved AS4/3501-6 composites and T800H/3900-2 composite. Note that the impact force depends on the target stiffness (thickness), thus both AS4/3501-6_IN and T800/3900-2 composite laminates experienced greater impact force; one reason is the larger thickness of the interleaved specimens (2.18 and 2.95 versus 2.13 mm).

The c-scanned imagery for plain and interleaved AS4/3501-6 is shown in Fig. 7 for both $H = 38.1$ and 50.8 mm. For $H = 38.1$ mm,

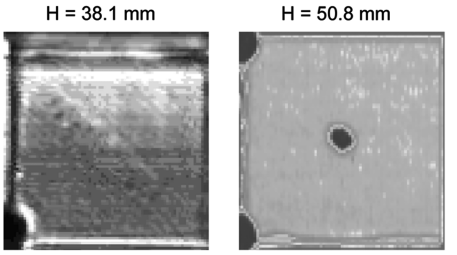

a) AS4-3501-6 Composites

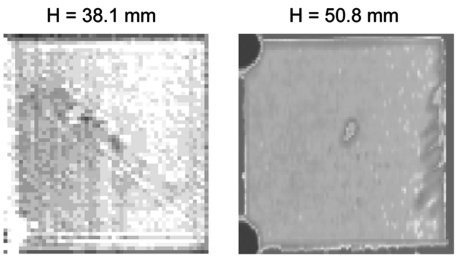

b) AS4-3501-6_IN Composites

Fig. 7 C-scan data for plain and interleaved composite laminates for two different impact heights.

there was no damage in either specimen. However, both specimens showed different amounts of damage at $H = 50.8$ mm. Areas of the damage were measured using image analysis and were listed in Table 1. The damage area of the interleaved laminate is about one-third of the damage area of the plain laminate. The plain AS4/3501-6 showed a significant delamination and matrix cracks, whereas the interleaved laminate showed no delamination, as shown in Fig. 8. In summary, electrospun Nylon-66 nanofiber interleaving reduced the impact damage to one-third or increased the impact damage resistance by 3 times compared to noninterleaved AS4/3501-6 composite with about 1.4% increase in thickness or added weight of nanofibers. Therefore, nanofabric interleaving has the potential to decrease impact damage or increase damage resistance with minimal increase in the thickness or weight.

C. Mode I Fracture and Delamination Onset Life

The energy release rate G_I versus delamination extension da for plain and interleaved AS4/3501-6 composites was plotted in Fig. 9. Hollow symbols represent plain specimens, whereas solid symbols represent interleaved specimens. Different symbol types represent

Table 1 Comparison of impact performance of AS4/3501-6 (plain and interleaved) and T800H/3900-2

Impact Parameter		AS4/3501-6	AS4/3501-6_IN	T800H/3900-2
Plate Thickness, mm		2.13	2.18	2.95
$H = 38.1$ mm	Max force, N	951	1,060	1,320
	Duration, ms	1.16	1.14	0.92
	Impact energy, J	0.47	0.47	0.47
	Damage area, mm^2	0.0	0.0	0.0
$H = 50.8$ mm	Max force, N	1,020	1,560	1,850
	Duration, ms	1.38	1.08	0.90
	Impact energy, J	0.80	0.80	0.80
	Damage area, mm^2	84.4	27.5	0.0

Table 2 G_{IC} and G_{IR} of plain and interleaved AS4/3501-6 composites and the comparison with T800H/3900-2

	AS4/3501-6		Toray [14]	
Mode I fracture toughness, J/m^2	Plain	Interleaved	T800H/3631 Base	T800H/3900-2 Interleaved
G_{IC}	84	212	180	710
G_{IR}	154	201	250	280

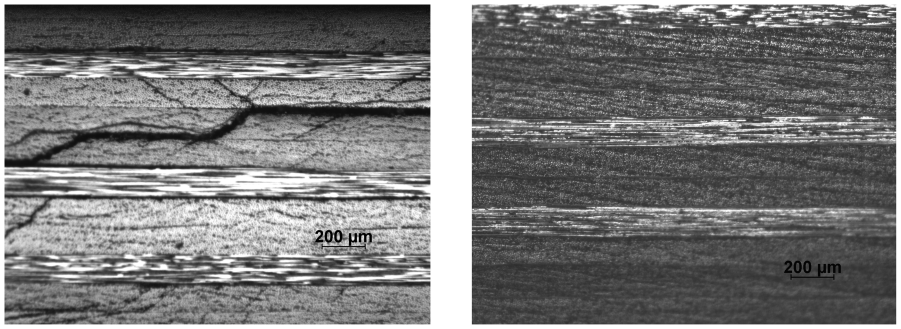

a) Plain AS4/3501-6 b) Interleaved AS4/3501-6

Fig. 8 Comparison of through-the-thickness impact damage at the center of the test section for impact height of 50.8 mm.

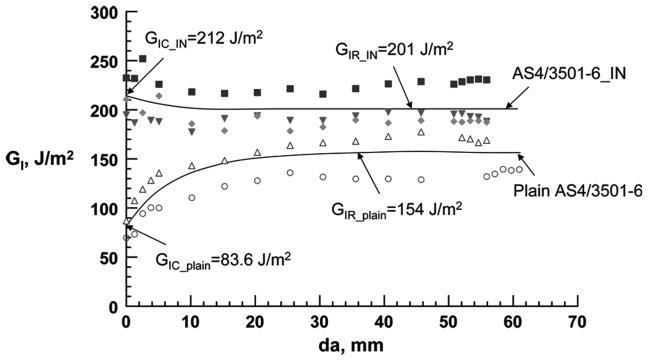

Fig. 9 Fracture toughness and resistance of plain and interleaved AS4/3501-6 composites.

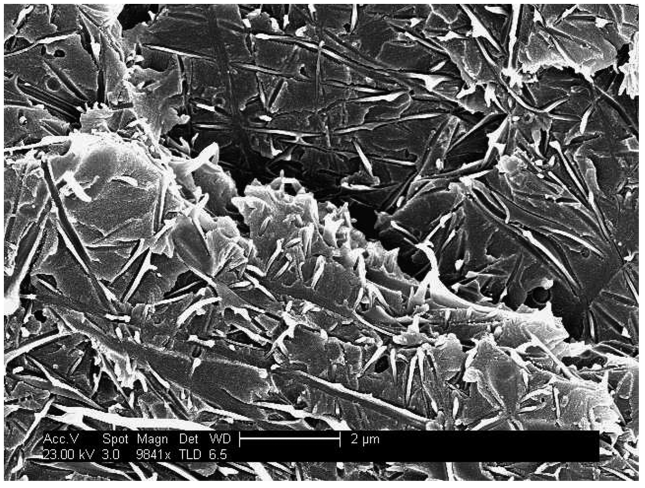

Fig. 10 SEM image of the fracture surface of the nanofabric interleaved AS4/3501-6 specimen.

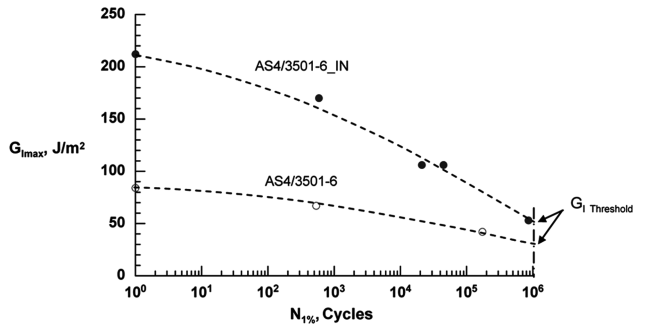

Fig. 11 $G_{I\max}$ versus fatigue onset life for plain and interleaved AS4/3501-6 composites.

different test specimens (two for plain and three for interleaved). Table 2 lists the initiation fracture toughness G_{IC} and the fracture resistance G_{IR} of plain and interleaved AS4/3501-6 composites and the commercial T800H/3631 composites [14]. The average initiation fracture toughness G_{IC} of plain and interleaved AS4/3501-6 is 84 and 212 J/m^2, respectively, about a 150% increase. For plain AS4/3501-6, the fracture resistance increased with the delamination propagation and reached a constant value of about 154 J/m^2 after 25 mm of delamination propagation. On the other hand, interleaved AS4/3501-6's resistance decreased with delamination growth and leveled off at about 201 J/m^2, an increase of about 30% over the plain AS4/3501-6 laminate. These percentage increases of G_{IC} and G_{IR} are on the same order as those of T800H/3900-2 when compared with its noninterleaved T800H/3631 composite [14] (see Table 2) but with no penalty on thickness increase. Figure 10 shows the SEM image of the fracture morphology of the nanofabric interleaved AS4/3501-6 specimen. Stretching, separation, and breakage of Nylon-66 nanofibers can be seen on the specimen surface, which are the reasons for toughness enhancement.

Two plain specimens ($G_{I\max} = 67$ and 42 J/m^2) and four nanofabric interleaved specimens ($G_{I\max} = 170$, 106, and 53 J/m^2) were tested for delamination onset lives for $R = 0.3$. Figure 11 shows $G_{I\max}$ versus delamination onset life $N_{1\%}$ for the two materials. Notice the wide separation between the two curves, which signifies the impact of nanofabric interleaving on the fatigue onset life. Onset threshold $G_{I\,\text{threshold}}$ ($G_{I\max}$ at $N = 10^6$ cycles) values of plain and nanofabric interleaved AS4/3501-6 are 30 and 50 J/m^2, respectively, which is an increase of 67%.

V. Conclusions

The concept of electrospun polymer nanofiber fabric interleaving to enhance dynamic properties, impact damage resistance, fracture toughness and resistance, and delamination onset life was evaluated. Polymer nanofabric interleaving increased the laminate thickness and weight by an order of 1%, and its impact on in-plane mechanical properties of the composite laminate would be statistically zero. On the other hand, its influence on interlaminar fracture toughness and resistance, impact damage resistance, and damping is substantial. Results of this study showed that interleaving AS4/3501-6 composite laminate increased the damping by 13%, reduced the impact damage size to one-third, increased fracture toughness and resistance by 1.5 times and one-third, respectively, significantly increased delamination onset life, and increased $G_{I\,\text{threshold}}$ by two-thirds. These improvements are comparable to that of the commercial T800H/3900-2 composites but with no thickness increase penalty, loss of in-plane properties, or multiple glass transition temperatures.

Acknowledgments

The authors wish to acknowledge the financial support of the U.S. Army Research Office grant no. W911NF0410176 and U.S. Army Research Laboratory–Micro Autonomous Systems and Technology grant no. W911NF-08-2-0004. They also acknowledge the support of the U.S. Office of Naval Research grant no. N00014-07-1-0465.

References

[1] O'Brien, T. K., "Towards a Damage Tolerance Philosophy for Composite Materials and Structures," American Society for Testing and Materials Special Technical Publication, No. 1059, 1990, p. 7.

[2] Pagano, N. J., *Interlaminar Response of Composite Materials*, Composite Materials Series, Vol. 5, Elsevier, Amsterdam, 1989.

[3] Salpekar, S. A., O'Brien, T. K., and Shivakumar, K. N., "Analysis of Local Delaminations Caused by Angle Ply Matrix Cracks," *Journal of Composite Materials*, Vol. 30, No. 4, 1996, pp. 418–440.

[4] Chan, W. C., "Design Approaches for Edge Delamination Resistance in Laminated Composites," *Journal of Composites Technology and Research*, Vol. 13, No. 2, 1991, pp. 91–96.

[5] O'Brien, T. K., "Delamination Durability of Composite Materials for Rotorcraft," NASA/Army Rotorcraft Technology, NASA CP 2495, 1988, pp. 573–605.

[6] Browning, C. E., and Schwartz, H. S., "Delamination Resistant Composite Concepts," *Composite Materials: Testing and Design*, edited by J. M. Whitney, American Society for Testing and Materials Special Technical Publication No. 893, 1986, pp. 256–265.

[7] Odagiri, N., Muraki, T., and Tobukuro, K., "Toughness Improved High Performance Torayca Prepreg T800H/3900 Series," *Proc. 33rd Int. SAMPE Symp.*, Society for the Advancement of Material and Process Engineering, Covina, CA, 1988, pp. 272–283.

[8] Pagano, N. J., and Pipes, R. B., "The Influence of Stacking Sequence on Laminate Strength," *Journal of Composite Materials*, Vol. 5, No. 1, 1971, pp. 50–57.
doi:10.1177/002199837100500105

[9] Mignery, L. A., Tan, T. M., and Sun, C. T., *The Use of Stitching to Suppress Delamination in Laminated Composites*, American Society for Testing and Materials Special Technical Publication No. 876, 1985, pp. 371–385.

[10] Dow, M. B., and Dexter, H. B., "Development of Stitched, Braided and Woven Composite Structures in the ACT Program and Langley Research Center," NASA TP-97-206234, Nov. 1997.

[11] Howard, W. E., Gossard, T., Jr., and Jones, R. M., "Reinforcement of Composite Laminate Free-Edges with U-Shaped Caps," AIAA Paper No. 86-0972, 1986.

[12] Chan, W. S., and Ochoa, O. O., "Edge Delamination Resistance by a Critical Ply Termination," *Key Engineering Materials*, Vol. 37, 1989, pp. 285–304.
doi:10.4028/www.scientific.net/KEM.37.285

[13] Masters, J. E., "Improved Impact and Delamination Resistance Through Interleafing," *Key Engineering Materials*, Vol. 37, 1989, pp. 317–348.
doi:10.4028/www.scientific.net/KEM.37.317

[14] Hojo, M. Matsude, S., Tanaka, M., Ochiai, S., and Murakami, A., "Mode I Delamination Fatigue Properties of Interlayer-Toughened CF/Epoxy Laminates," *Composites Science and Technology*, Vol. 66, No. 5, 2006, pp. 665–675.
doi:10.1016/j.compscitech.2005.07.038

[15] Formhals, A., "Method and Apparatus for Spinning," U.S. Patent No. 2160962, 1939.

[16] Ko, F. K., "Nanofiber Technology: Bridging the Gap Between Nano and Macro World," *NATO ASI on Nanoengineered Nanofibrous Materials*, Kluwer Academic, Norwell, MA, 2004.

[17] Shivakumar, K., and Lingaiah, S., "Ultra Lightweight Materials for Bio-Inspired Microsystems," *Proceedings of 16th International Conference on Composite Materials (ICCM-16)*, Japan Society of Composite Materials, Tokyo, July 2007.

[18] Lingaiah, S., Shivakumar, K. N., and Sadler, R. L., "Electrospinning of Nylon-66 Polymer Nanofabrics," AIAA 2008-1787, April 2008.

[19] Takeda, N., and Ogihara, S., "Micromechanical Characterization of Local Deformation in Interlaminar-Toughened CFRP Laminates," *Composites, Part A: Applied Science and Manufacturing*, Vol. 29A, No. 12, 1998, pp. 1545–1552.
doi:10.1016/S1359-835X(98)00067-0

[20] Swaminathan, G., and Shivakumar, K., "A Re-Examination of DMA Testing of Polymer Matrix Composites," *Journal of Reinforced Plastics and Composites*, Vol. 28, No. 8, 2008, pp. 979–994.
doi:10.1177/0731684407087740

[21] Lal, K. M., "Low Velocity Transverse Impact Behavior of 8-Ply, Graphite-Epoxy Laminates," *Journal of Reinforced Plastics and Composites*, Vol. 2, No. 4, 1983, pp. 216–225.
doi:10.1177/073168448300200401

[22] Meirovitch, L., *Elements of Vibration Analysis*, McGraw-Hill, New York, 1975, p. 212.

[23] ASTM Standard D5528-94a, "Standard Test Method for Mode I Interlaminar Fracture Toughness of Unidirectional Fiber-Reinforced Polymer Matrix Composites," *Annual Book of ASTM Standards*, Vol. 15.03, American Society for Testing and Materials, Philadelphia, 1999, pp. 283–292

[24] Hashemi, S., Kinloch, A. J., and Williams, J. G., "Corrections Needed in Double Cantilever Beam Tests for Assessing the Interlaminar Failure of Fiber Composites," *Journal of Materials Science Letters*, Vol. 8, No. 2, 1989, pp. 125–129.
doi:10.1007/BF00730701

[25] ASTM Standard D6115-97, "Standard Test Method for Mode I Fatigue Delamination Growth Onset of Unidirectional Fiber-Reinforced Polymer Matrix Composites," *Annual Book of ASTM Standards*, Vol. 15.03, American Society for Testing and Materials, Philadelphia, 1999, pp. 327–332.

[26] ASTM Standard E1640-04, "Standard Test Method for Assignment of the Glass Transition Temperature by Dynamic Mechanical Analysis," *Annual Book of ASTM Standards*, Vol. 14.02, American Society for Testing and Materials International, West Conshohocken, PA, 2004, pp. 562–566.

A. Roy
Associate Editor